JOURNAL OF GUIDANCE, CONTROL, AND DYNAMICS
Vol. 29, No. 3, May–June 2006

Comparison of Control and Display Augmentation for Perspective Flight-Path Displays

T. M. Lam,* M. Mulder,† M. M. van Paassen,‡ and J. A. Mulder§
Delft University of Technology, 2629 HS Delft, The Netherlands

Manually performed piloting tasks with a perspective flight-path display require considerable effort. To improve this, display augmentation is used: additional symbology such as a flight-path predictor is added. An alternative approach would be to use control augmentation, using fly-by-wire techniques to simplify the control task of the pilot. A control-theoretical analysis of different display and control augmentation concepts is presented. It is shown how design techniques for flight directors can be applied to the analysis of display augmentation. The different concepts have also been tested in a piloted experiment, conducted in a high-fidelity moving-base flight simulator. Experimental results confirm the findings from the control-theoretical analysis. Overall, the control augmentation concepts outperform the display augmentation concepts: Pilot workload and control activity are strongly reduced with equal or better performance. These benefits become more apparent as the task difficulty increases.

Nomenclature

g	=	gravitational acceleration, m/s^2
n_z	=	normal acceleration
T_p	=	predictor time, s
x_e, v_e, t_e	=	lateral, vertical, total position error, m
γ_e	=	climb angle error, deg
ΔT	=	control augmentation lag time, s
δ_{e_c}, δ_{a_c}	=	elevator, aileron control surface deflections, deg
δ_{e_s}, δ_{a_s}	=	elevator, aileron stick displacements, deg
θ, ϕ	=	pitch, roll attitude angle, deg
τ_e	=	effective information processing time delay, s
τ_N	=	neuromuscular lag time constant, s
φ_m	=	phase margin, deg
χ_e	=	track angle error, deg
Ω	=	turn rate, deg/s
ω_c	=	crossover frequency, rad/s

I. Introduction

RESEARCH indicates that perspective guidance displays such as the tunnel-in-the-sky have significant advantages over conventional flight displays.[1] They allow high-precision manual trajectory following,[2–6] improve pilot situation awareness,[7–9] and are compatible with a variety of other control and monitoring tasks.[10,11] Whether perspective guidance displays actually simplify the pilot control task is questionable, however. In the 1980s one of the main tunnel display pioneers, Grunwald,[5] already reported considerable difficulty for pilots in accurately tracking complex curved trajectories (Grunwald et al.[12]). Recent flight tests confirmed these findings.[13–16]

Presented as Paper 2004-5238 at the AIAA Guidance, Navigation, and Control Conference, Providence, RI, 16–19 August 2004; received 28 December 2004; revision received 14 March 2005; accepted for publication 14 March 2005. Copyright © 2005 by Technical University Delft. Published by the American Institute of Aeronautics and Astronautics, Inc., with permission. Copies of this paper may be made for personal or internal use, on condition that the copier pay the $10.00 per-copy fee to the Copyright Clearance Center, Inc., 222 Rosewood Drive, Danvers, MA 01923; include the code 0731-5090/06 $10.00 in correspondence with the CCC.

*Research Associate, Control and Simulation Division, Faculty of Aerospace Engineering, Kluyverweg 1; t.m.lam@lr.tudelft.nl.

†Associate Professor, Control and Simulation Division, Faculty of Aerospace Engineering, Kluyverweg 1; m.mulder@lr.tudelft.nl. Member AIAA.

‡Associate Professor, Control and Simulation Division, Faculty of Aerospace Engineering, Kluyverweg 1; m.m.vanpaassen@lr.tudelft.nl.

§Professor, Chairman of the Control and Simulation Division, Faculty of Aerospace Engineering, Kluyverweg 1; j.a.mulder@lr.tudelft.nl. Member AIAA.

Inspired by research on teleoperating unmanned aerial vehicles,[17] Grunwald decided to augment the display with additional symbols such as the flight-path vector (FPV) and the flight-path predictor (FPP)[5,18] (also Grunwald et al.[12]). The FPV explicitly shows the aircraft direction of motion in the world, allowing pilots to perceive this important variable directly, instead of deriving it through perceptual processing.[19] The FPP shows the aircraft future position, a couple of seconds ahead in time, with respect to a reference frame moving ahead of the aircraft, allowing the pilot to anticipate oncoming trajectory changes. The tunnel-and-predictor concept improves path-following performance and has become the standard in perspective flight-path displays.[6,20–25] The application of such techniques is called display augmentation. Its underlying principle is similar to the workings of a flight director. The feedback paths of the different loops of the pilot's guidance task are combined in the display presentation, leaving the pilots with equivalent dynamics that are relatively simple to control.[26]

A different, less actively pursued way to improve the performance of pilots and to reduce workload with perspective guidance displays is control augmentation, using techniques that have become feasible with the introduction of fly-by-wire (FBW) technology.[27–30] In this approach, the inner loops of the pilot's guidance task are closed by the control augmentation system (CAS), allowing the pilot to manipulate directly aircraft states higher in the control hierarchy. In particular a flight-path oriented CAS, that is, one that allows pilots to control directly the aircraft direction of motion, has proven to be a promising concept.[26,31]

From the preceding paragraph, one may conclude that (tunnel) display augmentation, as well as control augmentation concepts, aid pilots in controlling their aircraft along curved trajectories. The goal of this paper is to compare the benefits of these concepts in a systematic, control-theoretical as well as an experimental fashion. The paper is structured as follows. First, a theoretical analysis of both augmentation concepts is given. Second, these concepts are compared in an offline analysis, focusing on stability and performance characteristics. Third, an experiment to investigate pilot workload, performance and preferences with various augmentation concepts in a realistic setting was performed in a high-fidelity motion-base flight simulator. The experimental results are analyzed and compared to the results from the theoretical analysis.

II. Basics of Augmentation

When the tunnel display is used without any form of augmentation, the pilot perceives the aircraft motion from the changing tunnel perspective, the geometry in motion.[22,26,32] The pilot acts as a multiloop feedback control mechanism closing the loops of aircraft attitude (the inner loop), flight path (the middle loop), and position (the outer loop)[26,32] (Figs. 1a and 2).

Grunwald's early experiments with a basic, that is, not augmented, tunnel display revealed considerable performance limitations due to badly damped pilot responses, accompanied by a considerable level of workload, when flying complex curved trajectories.[5,12] He attributed these problems to the use of only a small-sized computer screen to present the optical information. Because of the lack of peripheral vision, the rate cues providing system damping could not be perceived appropriately. (With an average viewing distance of 0.80 m in front of a square screen with a diagonal of 8 in., a field of view of approximately 10 deg is provided, stimulating only the pilot's foveal vision.) In later studies, it was shown that, although pilots are indeed able to see where they are going, that is, their flight path, using the tunnel display alone, this perceptual process takes some time, resulting in processing lags that can be in the order of 500 ms or more.[19]

With display augmentation, symbology is added to the display that can be used by the pilot in closing the control loop, substituting or supplementing the other aircraft output variables that can be perceived from the display. Required control inputs remain the same, but the display cues simplify the pilot's task. Numerous investigations on the usefulness of such synthetic symbols have been conducted in the past in two-dimensional[33,34] and three-dimensional[4–6,12,17,35] aircraft guidance displays. An alternative is control augmentation, which works by changing the perceived aircraft dynamics. Figure 1 shows the two augmentation principles in relation to the baseline configuration. For a detailed discussion on the augmentation concepts, see Mulder.[26]

A. Equivalent Dynamics

With display augmentation, for example, when presenting an FPP symbol (Fig. 1b), the pilot should be able to change control strategy toward controlling just this symbol on the display. The relationship between what the pilot perceives, the FPP-output y, and the pilot actions, the aircraft control input u, is $H_{ac}H_{fpp}$, the equivalent dynamics, with H_{fpp} the dynamics of the FPP. Hence, by the choice of the predictor dynamics, the equivalent dynamics can be modified: The display augmentation dynamics can be designed effectively to cancel out part of the aircraft dynamics, reducing the order of the system to be controlled, preferably down to a single integrator over a wide frequency range.[26]

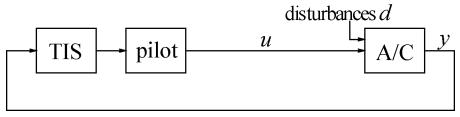

a) Baseline control situation

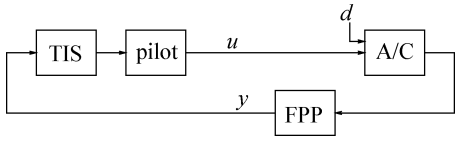

b) Display augmentation with FPP

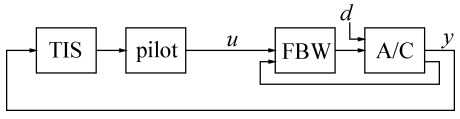

c) Control augmentation with FBW

Fig. 1 Three simplified augmentation forms, for control of aircraft (A/C) with TIS display; u, y and d are pilot control input, aircraft output, and disturbance (e.g., turbulence) acting on A/C, respectively.

With control augmentation (Fig. 1c), a control augmentation system effectively closes one (or more) of the aircraft feedback loops. The pilot's control deflection is now interpreted as a command or reference, and the CAS generates the appropriate control inputs.[36] With the CAS dynamics given by H_{fbw}, the equivalent dynamics become $H_{fbw}H_{ac}/(1+H_{fbw}H_{ac})$. Hence, the control system may be designed to, from the pilot's perspective, obtain an ideal command/response relationship.

Thus, when a pilot performing a target-following task is considered, such as following a prescribed reference trajectory, the augmentation principles are comparable in that they modify the equivalent dynamics of the controlled system.

B. Disturbance Rejection

On the augmented display, the response of the FPP will reflect the pilot input u and the atmospheric disturbances d, $y = H_{ac}(u+d)$, and the pilot must compensate for all disturbances. An accompanying problem is that, as the intensity of the atmospheric turbulence increases, the higher-frequency components will start to dominate the FPP response, reducing its effectiveness in the manual control loop.[17,19]

With control augmentation, the aircraft response is still a function of the pilot input u and the disturbance d. However, because the CAS closes (some of) the aircraft feedback loops, it suppresses the effects of disturbances considerably because their effect on the aircraft output y is governed by the dynamics $H_{ac}/(1+H_{fbw}H_{ac})$. Hence, a high bandwidth of the CAS may be designed to not only result in a desired command/response relationship ($y \approx u$), but also to mitigate the effects of disturbances acting on the aircraft.

In conclusion, the advantage of control augmentation over display augmentation is the disturbance rejection, expected to yield a substantial reduction of pilot workload.[26–28] Surprisingly, until now there has not been a systematic comparison between the two approaches, and the tunnel-and-predictor concept has become the de-facto standard in perspective flight-path displays.

III. Display Augmentation

The benefits of the augmented displays can be understood using three principles.[26,37] First, a well-designed display augmentation transforms the control task from a cognitive to a perceptual one. Second, it provides a means of establishing or improving the compatibility between the display and the pilot's mental model. Third, as discussed in the preceding section, display augmentation can effectively change the equivalent dynamics of the system to be controlled in a particular task context. These three principles will be elaborated in the sequel, in which the three main forms of display augmentation, providing synthetic command, status, and predictive information, respectively, will be introduced.[26]

A. Augmenting the Display

1. *Augmenting with Command Information: Flight Director*

The flight-director (FD) is an example of augmenting the conventional primary flight display with command information. Based on

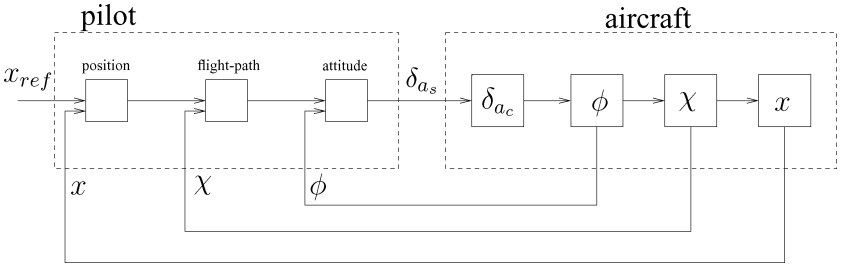

Fig. 2 Baseline control (equals to control with FPV) for lateral flight dynamics, where δ_{a_c} is actuator dynamics.

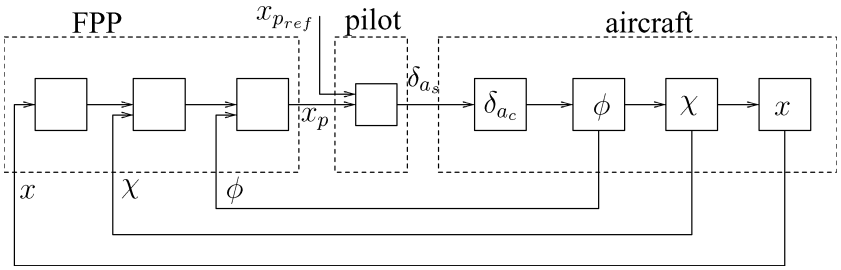

Fig. 3 FPP control, for lateral flight dynamics.

the requirements of the guidance task, the pilot selects an FD control mode and defines the controller set points. The FD computer algorithm then integrates the information and generates two control signals, one for the vertical and one for the lateral aircraft control channel, that are appropriate at that time. However, instead of feeding these control signals to the aircraft, which would make it an automatic pilot, these signals are presented on the display using FD command bars. The pilot must now move the control manipulator in such a way to keep the FD bars central on the artificial horizon display, that is, resulting in a two-axis compensatory tracking task.

The advantage of the FD is that the integration of information is conducted by the FD algorithm, relieving the pilot from this demanding cognitive task. The three feedback loops of Fig. 2 are closed automatically, and the appropriate control action is shown on the display. However, these FD command bars lack a clear meaning regarding the aircraft's spatiotemporal situation when shown into a perspective display; they bear no relationship to the pictorial world, they are not compatible with the pilot mental model, and they do not enhance situation awareness.[2,7,8] Hence, the FD meets the first and third principles stated earlier, but it does not support the second one.

Although certainly applicable in the present context, and although some have tried to integrate the FD with the perspective flight-path display,[10] we consider it a doubtful combination of concepts. Therefore, in the sequel we will concentrate on the symbology that is compatible with the pictorial tunnel display format and, therefore, compatible with a pilot's mental model.

2. *Augmenting with Status Information: FPV*

The FPV has become a standard feature of the modern glass cockpit primary flight display and the head-up display.[38] It shows the aircraft direction of motion relative to the ground and has proven to be very useful in ground-referenced aircraft maneuvering tasks.[34] This symbol shows status information, that is, the velocity vector tangential to the locally curved trajectory, and does not provide predictive information, except perhaps during rectilinear flight, nor does it tell the pilot what to do. It only makes the instantaneous direction of motion explicit on the display. Without the FPV, pilots must perceive the direction of motion through the optical flow generated by the changing tunnel perspective. Although humans are well equipped to perceive this variable from optical flow, several studies have indicated that significant processing lags are involved, limiting pilot performance.[19,22,32,39] With the FPV, the pilot can directly perceive the aircraft direction of motion, reducing the processing lags involved in perceiving this important state variable to zero.

Concerning the three principles of display augmentation, it is clear that the FPV meets the first two principles. However, the FPV does not add any dynamics to the control task; it is not expected to change the pilot baseline control strategy in Fig. 2. Controlling the aircraft still requires a feedback of attitude, flight path, and position. The third principle is, therefore, not supported.

3. *Augmenting with Predictive Information: FPP*

The FPP shows the aircraft's predicted position with a two-dimensional[6,12] or three-dimensional[5] symbol together with a highlighted reference frame at some time T_p ahead. The pilot task is to minimize the future aircraft lateral and vertical position errors by keeping the predictor symbol in the center of a reference frame (Fig. 3), resulting in a two-axis pursuit tracking task. Pursuit tracking is generally found superior over compensatory tracking in terms of performance and workload.[40] Even better, the perspective tunnel geometry allows a preview of the future trajectory changes, and, therefore, the future motion of the predictor reference frame, yielding an almost ideal task from a manual control point of view: pursuit tracking with preview.[40,41]

As shown in Fig. 3, the FPP prediction algorithm integrates the aircraft attitude, flight path, and position states relative to the nominal trajectory to generate a prediction of the future position (x_p in Fig. 3). When attempting to keep this future position close to the desired future position marked by the predictor reference frame ($x_{p_{\text{ref}}}$ in Fig. 3), the pilot effectively closes the three baseline feedback control loops. Hence, although the FPP does not explicitly tell the pilot what to do, as the flight director does; it involves an implicit command. That is, through showing what will happen in the near future when the current flight condition remains the same, that is, when the current pilot control input remains unchanged, it implicitly shows the pilot what to do. In addition, this implicit command is nicely integrated in the three-dimensional tunnel perspective. The FPP is the only concept that supports all three principles of display augmentation.

B. Tuning the FPP

The objective of this paper is to compare display and control augmentation concepts, and for a fair comparison, all augmentation concepts need to be tuned for optimal performance. The FPV symbol is not driven by a specific algorithm, and no parameters need to be adjusted to tune its performance. The FPP, however, is driven by a predictor algorithm, and this algorithm needs to be tuned to make it work optimally.[18]

1. *Choosing the Predictor Law*

The basic principle of the FPP is that a predictor symbol is shown at a distance $D = T_p V$ ahead, where T_p is the prediction time and V the airspeed. At the same distance D ahead, a cross section of the tunnel is highlighted: the predictor reference frame. The pilot's task is to keep the predictor in the predictor reference frame, that is, to reduce the difference between the lateral and vertical predicted position (x_p, v_p) and the reference frame position ($x_{p_{\text{ref}}}$, $v_{p_{\text{ref}}}$), a two-axis pursuit tracking task with preview.

Several algorithms are available to drive the predictor. Based on research on different predictor laws in the past,[6,18,20] it was decided to use the predictor based on the circular path assumption from Grunwald. In the circular path assumption, it is assumed that the vertical and lateral accelerations perpendicular to the flight path are constant, resulting in a future aircraft trajectory that is circular. Grunwald showed that for small accelerations the circular path assumption can be approximated by a second-order Taylor series expansion of the vehicle's lateral and vertical motion. That is, for the lateral predicted position one obtains (similarly for the vertical predicted position):

$$x_p(t + T_p) = x(t) + T_p \dot{x}(t) + T_p^2 \ddot{x}(t) \big/ 2 \tag{1}$$

Substituting $\dot{x} \approx V\chi$ and $\ddot{x} \approx g\phi$ (small-angle kinematics) into Eq. (1) exemplifies our earlier statement that when controlling the flight-path predictor symbol on the display the pilot effectively

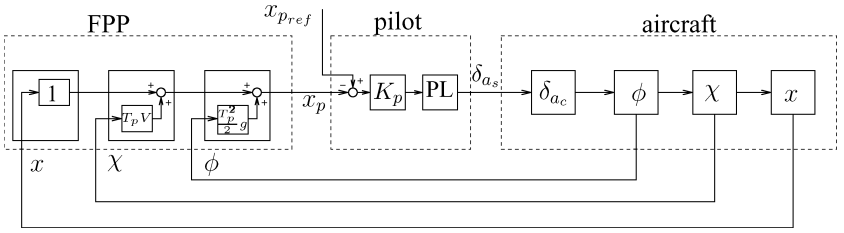

Fig. 4 Lateral closed-loop pilot–vehicle system with FPP; pilot limitations (PL) neuromuscular lag τ_N and time delay τ_e indicated.

closes the three baseline feedback loops of attitude ϕ, flight path χ, and position x (Figs. 3 and 4).

Laplace transforming Eq. (1) yields the lateral predictor dynamics $H_{\text{fpp}}(s)$, that is, $H_x^{x_p}(s)$, that will be cascaded with the lateral aircraft dynamics $H_{\text{ac}}(s) = H_{\delta_a}^{x}(s)$ to obtain the equivalent dynamics $H_{\text{ac}}(s)H_{\text{fpp}}(s)$:

$$H_{\delta_a}^{x_p}(s) = H_{\delta_a}^{x}(s)H_x^{x_p}(s) = \overbrace{H_{\delta_a}^{x}(s)}^{\text{aircraft}}\overbrace{\left(1 + T_p s + T_p^2 s^2/2\right)}^{\text{predictor}} \qquad (2)$$

Hence, the aircraft lateral dynamics $H_{\delta_a}^{x}(s)$ are supplemented by two complex zeros having a fixed damping $\sqrt{2}/2$ and a natural frequency that is a function of the prediction time, $\omega_0 = \sqrt{2}/T_p$.

2. *Effect of the Predictor*

Figure 4 shows the closed loop pilot–vehicle control system with the FPP. In the following analysis, a linear model of the Cessna Citation 500, a small business jet, will be used, with an indicated airspeed (IAS) of 59.9 m/s (Ref. 42). The aircraft is equipped with a yaw damper. The pilot is modeled as a gain K_p, a neuromuscular lag $\tau_N = 0.1$ s, and a time delay $\tau_e = 0.3$ s (Ref. 40).

The effect of the predictor on the open loop is that the transfer function describing the equivalent dynamics $H_{\delta_a}^{x_p}(s)$ between the stick deflection δ_a and the predicted position x_p has an integrator-like characteristic over a certain frequency interval. Figure 5a, showing the magnitude of the open loop for prediction times ranging from $T_p = 1$ to 9 s, shows that this frequency interval depends on the prediction time. A small prediction time yields a higher break frequency, which in turn leads to a small interval and vice versa. At approximately 4 rad/s, the open loop becomes a second-order integrator for all prediction times. Sachs introduced roll rate feedback to the predictor algorithm to extend the integratorlike interval to a higher frequency range in the lateral motion.[6] Similar improvement was gained for the longitudinal dynamics using the pitch rate.

The effect of the predictor on the closed-loop pilot–vehicle–predictor system is that the closed-loop poles move toward the predictor zeros for higher pilot gains K_p. Figures 5b and 5c show a root locus plot as a function of K_p for prediction times T_p equal to 4 and 9 s, respectively. The closed-loop system is initially unstable due to the spiral divergence (SD) mode and, for both prediction times, becomes stable with increasing pilot gain. For $T_p = 4$ s the SD pole enters the left half-plane, yielding stability for $K_p = 0.39$, but again leaves the left half-plane for higher gains, $K_p > 0.78$. For $T_p = 9$ s, the SD pole also enters the left half-plane (stable when $K_p = 0.07$) into the direction of the predictor zero, and another closed-loop pole becomes unstable, $K_p > 0.50$. A small prediction time requires a larger pilot gain to stabilize the system, and in both cases, the system becomes unstable again for increasing pilot gains. To achieve a certain robustness for variations in the pilot gain, it is clear that a well-chosen prediction time is important for pilot performance and workload. For this reason a search for the optimal prediction time appears to be worthwhile.

3. *Determining Optimal Prediction Time*

Grunwald introduced a method to find the optimal prediction time.[18] This time depends on the aircraft dynamics, the velocity, and the accuracy requirements of the piloting task. In the case of slow aircraft dynamics, a small prediction time will result in slow movement of the symbol that may not be adequate in anticipating

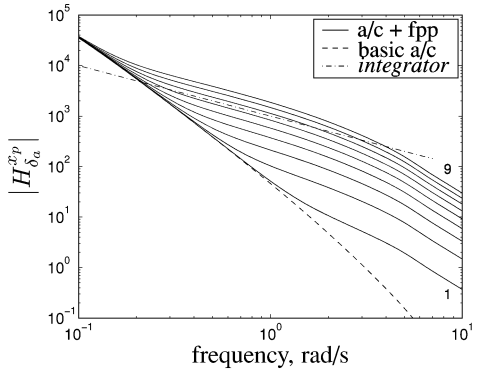

a) Magnitude of open-loop system $H_{\delta_a}^{x_p}$ for prediction times T_p 1–9 s: – – –, basic aircraft dynamics $H_{\delta_a}^{x}$

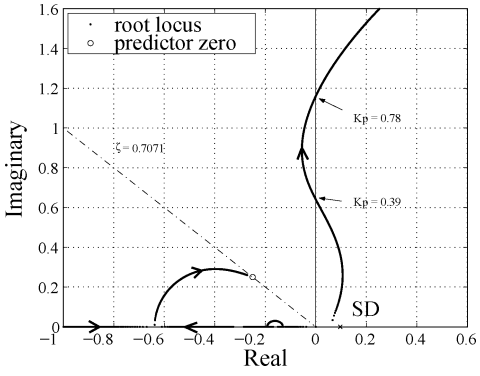

b) Root locus plot of pilot gain K_p ($T_p = 4$ s)

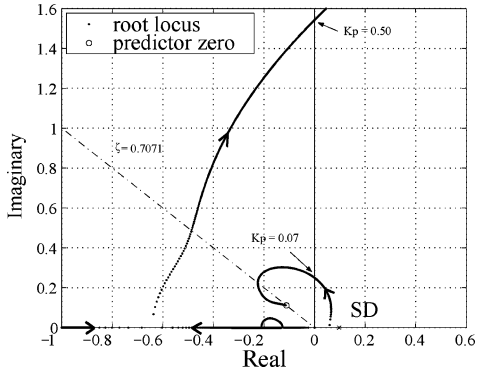

c) Root locus plot of pilot gain K_p ($T_p = 9$ s)

Fig. 5 Effect of predictor on open-loop and closed-loop pilot-vehicle system (lateral dynamics).

oncoming changes of the trajectory. In case of fast dynamics, a large prediction time results in a rapidly moving symbol that may be difficult to control.[17]

When the aircraft dynamics and velocity are fixed, the optimum prediction time depends on the size of the initial position deviation with respect to the nominal trajectory. Grunwald[18] claimed that the best gain as a function of T_p is the minimal gain required to settle the position deviation within 5% of the original deviation within 60 s. In the present study, a stricter rule was used, namely, a settling within

5% in less than 15 s. The initial deviation was chosen to be 25 m, one-half of the tunnel width used in the experiment.

For the Cessna Citation used here, the optimal prediction time for the lateral dynamics was found to be 6 s, whereas for the vertical dynamics the optimal time was 2 s. These prediction times will be used for the analytical comparison with the control augmentation, as will be discussed in the next sections.

IV. Control Augmentation Principles

A. Attitude-Oriented and Flight-Path Oriented Control Augmentation

An earlier study[26] investigated the compatibility of two FBW control laws, attitude-oriented control and flight-path-oriented control, with the perspective flight-path display. In the attitude-oriented concept, the pilot control inputs act as attitude-rate (that is, pitch-rate and roll-rate) commands: When the pilot control input is zero, the FBW computer maintains the instantaneous attitude. Here, the inner loop of aircraft control, attitude, is automatically controlled. With the flight-path-oriented concept, the pilot control inputs act as FPV rate (that is, climb-angle rate and track-angle rate) commands, or, in other words, the pilot commands the aircraft direction of motion relative to the ground.[27] When the control input is zero, the instantaneous inertial flight path is maintained. In other words, the FBW computer does not only close the inner loop but closes the middle loop (flight path) as well (Fig. 6).

Both of the designs were evaluated in two pilot-in-the-loop experiments, one conducted in a fixed-base simulator[26] and one in a moving-base flight simulator.[43] These experiments showed that, in comparison to the baseline manual control, control augmentation significantly reduced pilot workload and at the same time improved path-following performance considerably. The flight-path-oriented concept outperformed the attitude-oriented design, with superior performance achieved with the lowest control activity and workload. The benefits of this concept were larger when task difficulty increased.

Several other studies, from the early NASA investigations,[44–46] work at Boeing[27,47] and other aircraft manufacturers to recent research conducted in the context of simplifying aircraft manual control for general aviation pilots[29,30,48] also showed the potential benefits of a flight-path-oriented flight control system, with or without the use of a perspective flight-path display.

B. Characteristics of Flight-Path Oriented Control Augmentation

The baseline perspective flight-path display can be easily augmented with an FPV symbol, significantly improving the perception of the aircraft direction of motion. The flight-path-oriented control system nicely complements this information by allowing the pilot directly to command the desired flight direction. Hence, the combination of this controller with the tunnel display yields a task-oriented control/display system, an attractive concept from the pilot perspective.[26]

The closed-loop pilot–FBW–aircraft system for the flight-path-oriented control law is shown in Fig. 7. The aircraft model and pilot model were similar to the FPP situation discussed earlier (Fig. 4). The discussion is limited to the lateral dynamics, similar arguments hold for the longitudinal case.

Figure 7 shows that the FBW computer closes the aircraft attitude and flight-path loops. The dotted block indicates that an attitude rate feedback can be used to increase stability, as has indeed been done here.

The pilot lateral control deflections are interpreted as track-angle rate commands. Integrating the track-angle rate yields the commanded track angle χ_c, which is shown to the pilot on the display through a second FPV symbol, the commanded FPV. The importance of showing not only the instantaneous aircraft flight path but also the commanded flight path has been convincingly shown in many earlier studies.[27,44,46,47]

The desired track angle χ_{ref} in Fig. 7 can be perceived from the perspective tunnel display. That is, in straight tunnel sections it is the vanishing point of the tunnel projection at infinity.[22] In curved trajectories, however, the reference track is much more difficult to perceive, which makes the accurate tracking of circular tunnel trajectories a hard task to accomplish.[49]

Bode diagrams for the open-loop lateral, χ/χ_c, and longitudinal, γ/γ_c, flight-path-oriented FBW control laws are in Figs. 8a and 8b, respectively. The crossover frequency ω_c and phase margin φ_m of the lateral controller equal 1.13 rad/s and 53 deg, respectively. For the vertical control law, they equal 1.6 rad/s and 36 deg, respectively. A previous study, involving the modeling and identification of pilot control behavior with a generic tunnel display, showed that these values are typical for the middle-loop closure of a small aircraft like the Cessna Citation.[32] Note that the vertical controller uses a feedforward loop to increase the speed of the inital response.

C. Remaining Issues

The three main issues with the flight-path-oriented FBW are, first, the awkward constant lateral control deflections during turns, second, the lagged response of the FBW controller, and third, the lack of a clear reference for pilots of where to put the commanded FPV in the tunnel. These problems occur primarily in the lateral

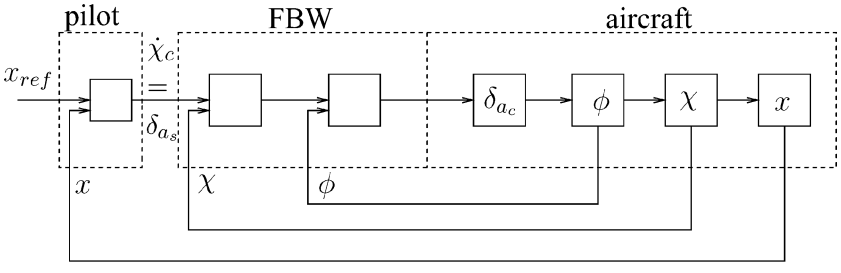

Fig. 6 FPV-oriented FBW control for lateral dynamics: compare with Figs. 2 and 3.

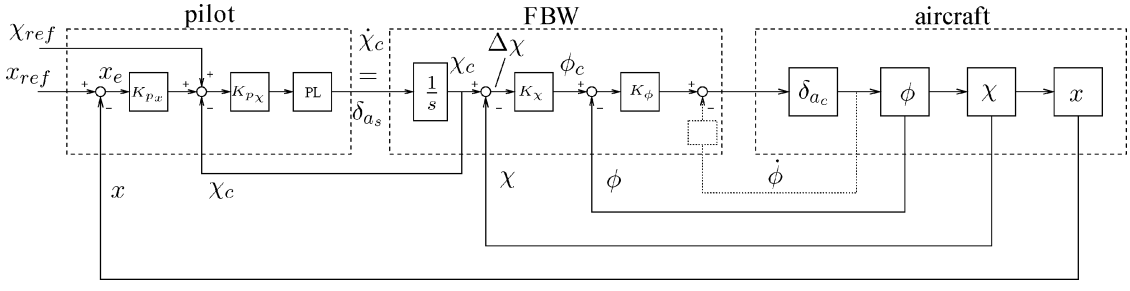

Fig. 7 Lateral closed-loop pilot–vehicle system block diagram with flight-path-oriented FBW.

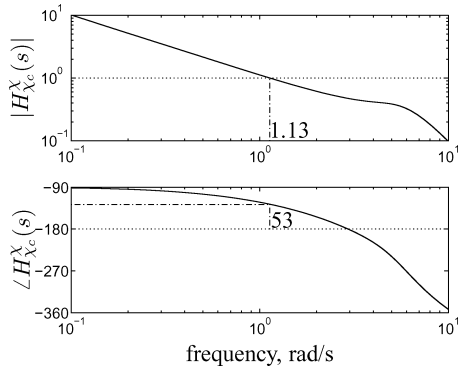

a) Lateral control law

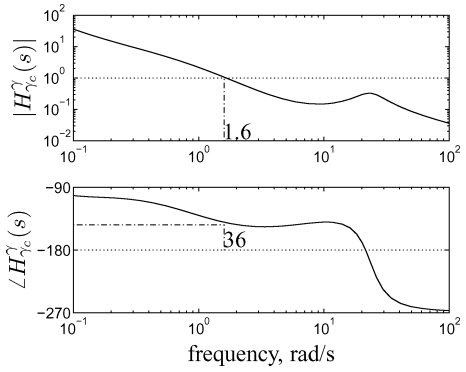

b) Longitudinal control law

Fig. 8 Bode diagrams of open-loop flight-path-oriented FBW control law.

aircraft maneuvering, in particular during turns. These issues are not important or do not occur at all in longitudinal maneuvers, where flight path γ needs to be changed.

1. Constant Control Deflections During Turns

In a turn, the direction of the aircraft track angle must change continuously at a rate commanded by the nominal trajectory curvature. With the implementation of the lateral flight-path-oriented control law in Fig. 7, this means that the track-angle rate $\dot{\chi}$ equals the reference rate $\dot{\chi}_{\text{ref}}$. Because the pilot lateral stick displacement is proportional to the commanded track-angle rate $\dot{\chi}_c$, the pilot must give a constant stick input to the left (right) in left (right) turns, a characteristic which may be quite unnatural for pilots, although accepted practice in car driving.

Studies revealed that pilots have more problems with exerting continuous forces during a sustained descent or climb rather than during a turn.[48,50,51] Still, pilots are not accustomed to this type of control.[26] A way to eradicate this problem would be to interpret the lateral control deflection δ_{a_s} as a curvature rate command, that is, a command on the rate of track-angle rate $\ddot{\chi}_c$. This would also require a different way of presenting the FPV, however, because the command is now a commanded curvature in three-dimensional space; for an example of this concept, see the work of Borst et al.[31]

2. Lagged Response of the Control Law

The open-loop combination of the FBW control law and the aircraft dynamics is a type 1 system for the response in track angle to the commanded track angle χ_c. In straight flight, with a constant χ_c, the steady-state error will, thus, be zero, but the system will experience a velocity error in a curve, when χ_c is linearly increasing. The pilot experiences this as a lagged response of the FBW control law. This lag affects performance, and because pilots are likely to compensate for it, this may contribute to workload.

For a stationary turn, and assuming that the inner-loop roll control system has a negligible roll-angle error, the velocity error $\Delta\chi$ for a certain aircraft turn rate Ω can be calculated from

$$\Omega = g\tan(K_\chi \Delta\chi)/V \tag{3}$$

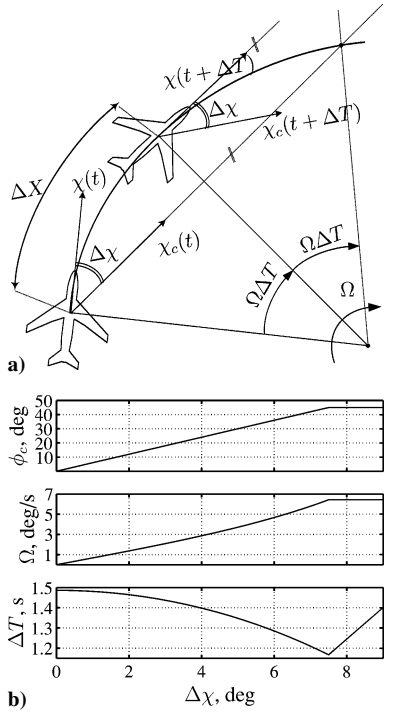

Fig. 9 Lateral FBW control law: a) top view of angular distance $\Delta X = \Delta T V$ in which aircraft track angle reaches commanded track issued at time t, i.e., $\chi(t+\Delta T) = \chi_c(t)$ and b) roll angle command ϕ_c, turn rate Ω, and lag time ΔT as function of ground-track-angle error $\Delta\chi(=\chi-\chi_c)$.

This velocity error can be expressed as a time lag, resulting in

$$\Delta T = \frac{V}{g}\frac{\Delta\chi}{\tan(K_\chi \Delta\chi)} \tag{4}$$

The relations between $\Delta\chi$ and ϕ_c, Ω, and ΔT are shown in Fig. 9b. Note that ΔT is not constant, due to the continuous changes of the track-angle error. Offline simulations showed that the track-angle error $\Delta\chi$ never exceeds 7 deg, which in turn results in small changes of ΔT (Ref. 42).

3. Lack of Reference for (Commanded) FPV

The FPV lies tangential to the aircraft trajectory, which is generally locally curved. In straight tunnels, this curvature is small, and there is no problem: Putting the FPV on the tunnel vanishing point results in a flight parallel to the nominal trajectory. However, in turns, the FPV is of lesser use because there is no clear, intuitive information about where the FPV would, ideally, be pointing. The pilot could look at a frame at some distance ahead and use it as a reference to direct the FPV. Taking a frame too far ahead, however, results in corner cutting, whereas looking too close may result in flying out of the curve.

The same holds for the FPV command symbol the pilot is controlling when operating with the flight-path-oriented FBW. As Fig. 9a shows, the situation is even worse here because there is also the lag between commanded track angle and the aircraft track angle.

An earlier study with the flight-path-oriented FBW revealed that, although training helped and in the end the pilot performance was quite satisfactory, pilots suggested that some reference should be shown of "where to put the commanded FPV" for optimal performance,[26] for example, through highlighting a frame moving ahead of the aircraft, similar to the FPP concept. This would appeal to the numerous investigations conducted on the application of a leading aircraft flying a perfect trajectory at some distance ahead serving as a guidance for the current FPV symbol.[34,52,53] However, for the flight-path-oriented FBW, the chosen distance ahead should take the lag time ΔT into account because it is the commanded FPV symbol that is being manually controlled instead of the current FPV.

Two possibilities exist for including the reference frame having a similar function as the leading aircraft mentioned earlier (Fig. 9a).

First, one could put the reference frame at an angular distance ΔX ahead, corresponding with ΔT. This frame then shows where in the tunnel ahead the aircraft track angle will have reached the track $\chi_c(t)$ commanded at that moment. Second, one could put the reference frame at an angular distance ahead that is twice as large, that is, at $2\Delta T$. This frame can then act as a target: Putting the commanded FPV in its center would result in the correct aircraft track angle ΔT later in time. This latter concept would result in a pursuit-tracking task similar to the FPP display augmentation, but now combined with the FPV-oriented control augmentation. In a later investigation, this concept, combining the best of two worlds has been demonstrated to perform satisfactory.[31] In the experiment presented here, however, only the first option has been tested.

V. Theoretical Analysis

In this section, the FPP display augmentation concept and the flight-path-oriented FBW control augmentation concept are compared through a theoretical model-based analysis. Path-following performance and control activity will be compared in the task of following a straight trajectory in the presence of atmospheric turbulence. Both concepts will be tuned to make them perform in an optimal fashion, and the investigation will focus on the sensitivity in stability and performance characteristics due to changes in these optimal settings. This allows us to analyze the robustness of the pilot–aircraft–augmentation system to variations in pilot control behavior.

A. Assumptions

In the analysis that follows, some important characteristics will be the same for the display augmentation (Fig. 4) and the control augmentation (Fig. 7). The aircraft model is a linear model of the Cessna Citation 500, flying at an airspeed of 59.9 m/s (116-kn IAS). It is equipped with a yaw damper to improve lateral stability and an autothrottle to keep the airspeed constant. The actuator dynamics are modeled as a first-order lag $[13/(s+13)]$. The atmospheric turbulence in both the lateral and longitudinal dimension is modeled as a Dryden spectrum (see Ref. 54) with scale length 300 m and intensity 2.25 m^2/s^2, and the wind is assumed zero.

The pilot model that is used depends on the augmentation concept. With the FPP, the pilot is a simple gain K_p (Fig. 4). With the FBW, the pilot is modeled with two gains, one closing the loop of the commanded FPV $K_{p\chi}$ and one closing the position loop K_{px}. For both concepts, the pilot limitations are modeled as a neuromuscular lag τ_N (0.1 s) and an information-processing time delay τ_e (0.3 s).

B. Stability and Performance of FPP

Performance and stability with the FPP depends on the prediction time T_p and the pilot gain K_p. For any particular prediction time, the magnitude of the pilot gain determines the crossover frequency and phase margin of the open-loop FPP control loop (lateral, x_p/δ_{a_s} and longitudinal, v_p/δ_{e_s}). Figure 10 shows the phase margin (stability), the position-tracking performance, and aircraft attitude variations for the lateral and longitudinal aircraft control, as a function of the prediction time T_p, for six levels of the crossover frequency (ranging from 0.5 to 1.3 rad/s). The values of these measures for the optimal prediction times (lateral, 6 s and longitudinal, 2 s) are shown as well.

The trends in the data are quite similar for both control dimensions. When a longer prediction time is chosen, the phase margins increase and attitude variations become smaller. Up to 2.5 s, the vertical position performance improves, whereas the lateral position performance decreases for larger prediction times. For a given prediction time T_p, when pilots increase their gain (resulting in higher crossover frequencies), the phase margin first slightly increases and then rapidly decreases, making the system unstable for gains that are too high. As expected, performance improves when pilots increase their gain, up to the point where the phase margins become too small.

The lateral phase margin is only 15 deg, which is rather small. It can be increased by including roll angle rate in the predictor law, as suggested by Sachs,[6] yielding a phase margin of about 35 deg, but this only marginally affected performance. The longitudinal phase margin of 57 deg is much better. As can be seen in Fig. 10, the optimal settings for the prediction times indeed correspond with a sensible compromise between stability (large phase margin) and performance (small position error).

C. Stability and Performance of Flight-Path-Oriented FBW

In the flight-path-oriented control augmentation concept, when fixing the design of the FBW control laws, the system performance and stability depends on the two pilot gains, in the lateral dimension $K_{p\chi}$ and K_{px} (Fig. 7). The pilot closes two loops, one feeding a desired flight path to the command flight-path symbol and one feeding a desired position to the desired flight path. These are referred to as the flight-path loop and the position loop, respectively.

Because the pilot control deflections are interpreted as flight-path rate commands, the effective dynamics in the fligh-path loop are first order, $K_{p\chi}/(s+K_{p\chi})$, and depend only on the gain $K_{p\chi}$. The bandwidth of this loop is smaller than the bandwidth of the FBW control law (lateral, 1.13 rad/s and longitudinal, 1.6 rad/s) and

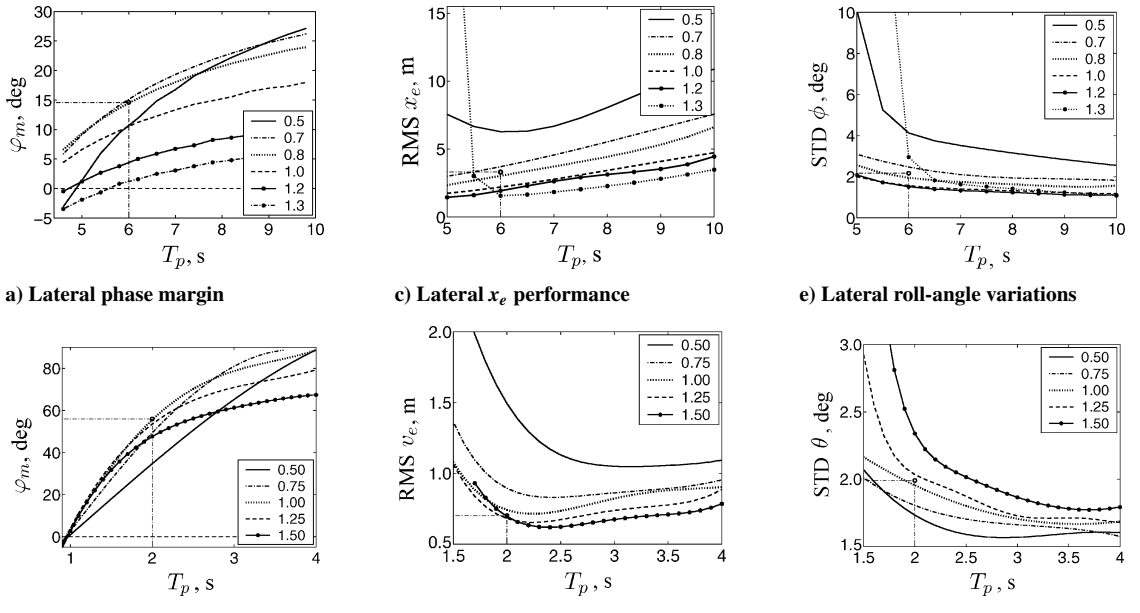

a) Lateral phase margin **c) Lateral x_e performance** **e) Lateral roll-angle variations**

b) Longitudinal phase margin **d) Longitudinal v_e performance** **f) Longitudinal pitch-angle variations**

Fig. 10 Lateral and longitudinal FPP phase margins, position-tracking performance, and attitude for range of prediction times T_p and pilot gains K_p (resulting in crossover frequencies in insets).

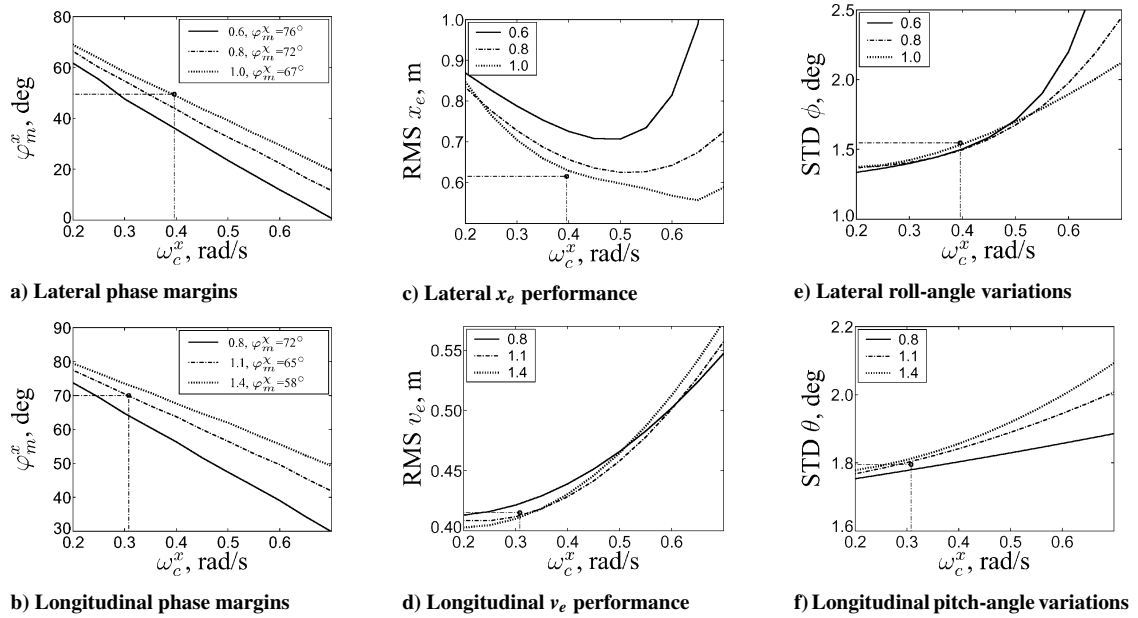

Fig. 11 Lateral and longitudinal flight-path-oriented FBW controller phase margins, position-tracking performance and attitude variations for range of commanded flight-path crossover frequencies ω_c^χ (insets) and position crossover frequencies ω_c^x.

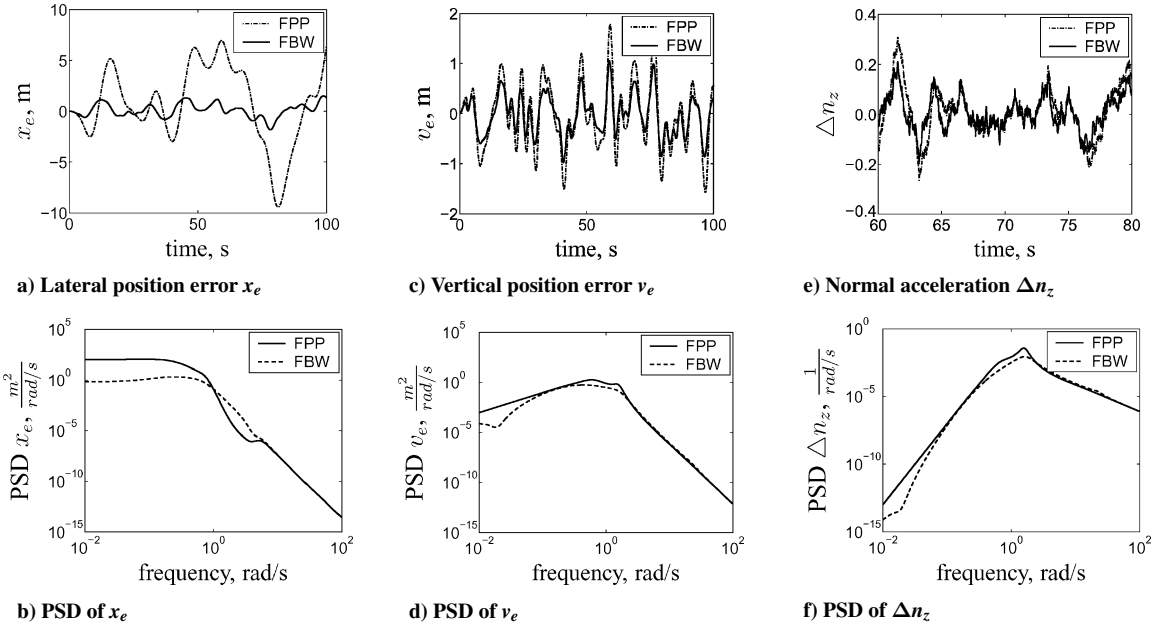

Fig. 12 Time histories and analytical PSD in disturbance rejection task, for optimally tuned FPV and FBW augmentation concepts.

depends only on the pilot flight-path gain, that is, $\omega_c^\chi \approx K_{p\chi}$. This loop serves the position loop, which is completely determined by the position loop gain K_{p_x}.

Figure 11 shows the lateral and longitudinal position loop phase margin φ_m^x, the position-tracking performance, and aircraft attitude variations, for three values of the flight-path crossover frequency ω_c^χ (insets, together with the flight-path loop phase margins) as a function of the position loop crossover frequency ω_c^x.

For the lateral control and longitudinal control, φ_m^x decreases almost linearly for increasing position loop crossover frequencies ω_c^x. The phase margin is larger when the flight-path crossover frequency ω_c^χ is larger, a typical result of a serial loop mechanism where an inner loop serves an outer loop. In the lateral control, clear minima can be found for the position-tracking performance, which lie independently of ω_c^χ at approximately $\omega_c^x = 0.4$ rad/s. In the vertical control dimension, such a minimum cannot be found. Rather surprisingly, performance increases when ω_c^x is smaller. Attitude variations in both lateral and vertical dimensions increase for higher crossover frequencies in the position control loop, whereas flight-path crossover shows mixed effects.

D. Discussion and Conclusions

When Figs. 10 and 11 are compared, it is seen that, first, the phase margins with the control augmentation are generally larger than with the display augmentation, indicating that the first is better capable of dealing with variations in pilot control behavior. Note, however, that the phase margins with the FPP can be increased through incorporating attitude rate in the predictor law. Second, in both dimensions, position-tracking performance is superior with control augmentation, accompanied with lower aircraft attitude variations: Control augmentation yields a more accurate and smoother ride.

Figure 12 shows typical time histories and analytical power spectral densities (PSD) for the tuned FPP and FBW augmentation concepts, confirming the superiority of the latter in this particular task. The better performance can be attributed that the FBW computer,

through closing the high-bandwidth inner and middle loops, automatically compensates for the effects of turbulence, whereas in the case of the FPP, the pilot closes all feedback loops integrated in the predictor symbol.

However, the task evaluated in this study was to follow a nominal trajectory that was straight, a disturbance task that emphasizes disturbance rejection. In the pilot-in-the-loop experiment discussed in the following sections, a complex, curved trajectory will be flown, where the emphasis lies more on path following. The FPP is expected to perform well this type of task, which could be better than the case for the flight-path-oriented control augmentation concept. In this sense, the experiment will complement the theoretical model-based analysis.

VI. Experimental Comparison

The goal of the experiment was to compare various control and display augmentation concepts for the tunnel display and to validate the results from the analytical study.

A. Method

1. Subjects and Instructions to Subjects

Six subjects participated in the experiment: four professional airline pilots, one retired airline pilot, and one test-pilot from the Control and Simulation Division (Table 1). The subjects were instructed to control the aircraft along the reference trajectory as accurately as possible.

2. Apparatus

Delft University's SIMONA Research Simulator (SRS) was used, a six-degrees-of-freedom high-fidelity moving-base flight simulator. The tunnel display was presented on a 15-in. liquid crystal display (LCD) screen 0.80 m in front of the subject. No outside visual was used. The control manipulators were an electrohydraulic control column and rudder pedals, both simulated with normal, that is, passive, characteristics.

3. Independent Variables

Four display and CAS combinations [augmentation concepts (AC)] and two levels of atmospheric turbulence (AT) were selected as the independent variables in the experiment (Fig. 13).

The first is baseline control with FPV (FPV), that is, the unaugmented control of the aircraft using elevator, aileron, and rudder deflections directly coupled to the control column and pedals. A green FPV symbol is presented on the display. This concept represents the baseline manual control situation shown in Fig. 2.

The second is (FPP), that is, the direct-link manual control, but now a green FPP symbol is presented, together with a yellow transparent predictor reference frame. This condition represents the tunnel-and-predictor concept shown in Fig. 3.

The third is flight-path-oriented FBW control (FBW), in which the pilot directly controls the direction of the aircraft motion (Fig. 6). The pilot stick displacements are interpreted by the FBW computer as climb-angle rate and track-angle rate commands. A green FPV symbol shows the instantaneous direction of motion; a yellow FPV symbol shows the commanded direction of motion.

Table 1 Characteristics of pilot subjects in experiment

Pilot	Age	Hours	Flying experience
A	31	2,100	Single engine, B747-400
B	64	13,100	Single engine, Cessna C550, DC3, DC8, F-28, B747-300/400
C	36	1,600	Single engine, Cessna C550, multiengine piston
D	52	12,790	Single engine, HFB 320 Hansa jet, DC9, MD11, MD80, A310, A320
E	31	2,200	Single engine, Light aircraft, Canadair Region Jet
F	37	5,550	Single engine, Cessna C500, B747-400, B767-300

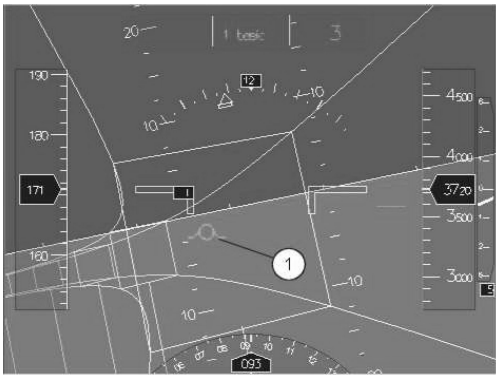

a) FPV display augmentation

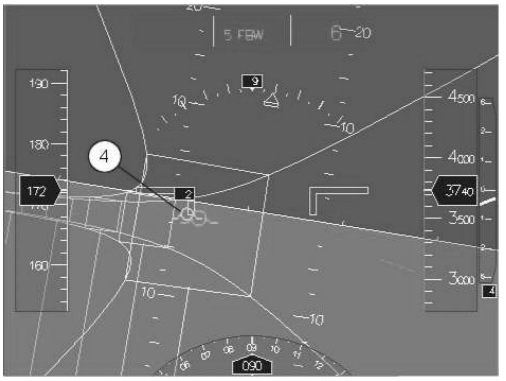

c) Flight-path-oriented control augmentation, FPV (green) and commanded FPV (yellow) (FBW)

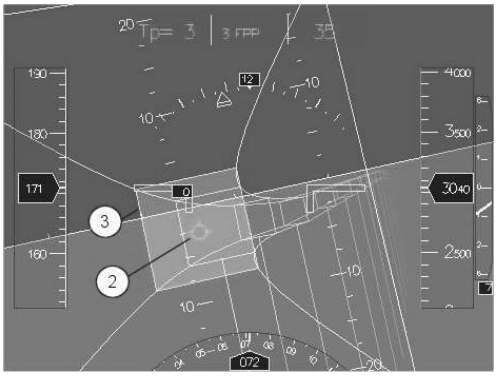

b) FPP display augmentation

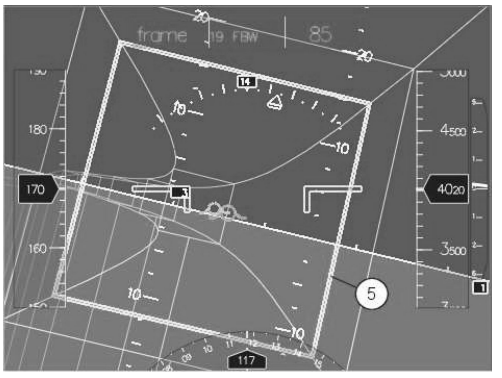

d) Flight-path-oriented control augmentation, with additional commanded FPV reference frame (FBW+)

Fig. 13 TIS displays with four augmentation concepts: 1) true FPV, 2) FPP, with 3) FPP reference frame, 4) commanded FPV, with 5) reference frame for the commanded FPV.

The fourth is flight-path oriented FBW control with reference frame (FBW+), that is, the same concept as the third-one, now with a highlighted yellow tunnel frame moving ahead of the aircraft ΔT seconds (the FBW controller lag time) ahead that acts as a control reference. The reference frame indicates where in the tunnel the true flight path will reach the commanded flight path.[42]

Because it was expected that the atmospheric disturbances would have different effects on the control and augmentation systems, two levels of AT were used.

4. Experiment Design and Procedure

A factorial within-subjects design was applied, resulting in 8 conditions (4 AC $\times$ 2 AT). Additionally, the nominal tunnel trajectory was mirrored with respect to a fictitious localizer plane to prevent pilot boredom and a task performance by rote.

Each pilot performed 4 blocks of 16 runs, 64 runs in total. Each block contained two randomly ordered replications of all 8 experiment conditions. The runs in the first block were used for training; the last 3 blocks (48 runs, i.e., all conditions 6 times) were used as the measurements. A single run lasted 4 min. After each run the pilot was asked to rate mental workload using the NASA Task Load Index (TLX) subjective rating scale.[55] After the experiment the pilots were asked to complete a questionnaire, addressing the usefulness of the augmentation techniques in conducting their task.

5. Dependent Measures

The path-following performance was expressed by the root-mean square of the aircraft lateral (x_e), vertical (v_e), and total [$t_e = \sqrt{(x_e^2 + v_e^2)}$] position errors and by the standard deviation (STD) of the aircraft lateral (χ_e) and vertical (γ_e) flight-path-angle errors. Pilot control activity was expressed by the STD of the lateral and the vertical stick deflection rates, $\dot{\delta}_{a_s}$ and $\dot{\delta}_{e_s}$, and the average number of control activities per unit of time (dacnt and decnt). Because the display and control augmentation concepts require different strategies in the lateral plane (where the FBW systems require a constant lateral control deflection in turns), the control deflections themselves were not used.

Ride comfort was expressed by the STD of the lateral and vertical accelerations $\ddot{x}_e$ and n_z. Aircraft-related variables such as the attitude ϕ and θ and the attitude rates $\dot{\phi}$ and $\dot{\theta}$ were also measured. Finally, the number of times the roll rate $\dot{\phi}$ exceeded a certain limit [$3 < \dot{\phi} < 5$ ($\dot{\phi}_{3-5}$), $5 < \dot{\phi} < 7$ ($\dot{\phi}_{5-7}$) and $\dot{\phi} > 7$($\dot{\phi}_{>7}$) deg/s] was counted to study the aggressiveness of the maneuver in the lateral plane. Similarly, in the vertical plane, it was counted how often the normal acceleration n_z exceeded certain values [$1.05 < n_z < 1.15$(Δn_{z_1}), $1.15 < n_z < 1.35$ (Δn_{z_2}) and $n_z > 1.35$ g (Δn_{z_3}) g]. Pilot workload was analyzed using the NASA TLX subjective workload rating.

B. Description of Experiment Simulation

A generic tunnel-in-the-sky (TIS) display was used with square tunnel frames, having a fixed size of 50 m. Figure 13 shows the displays corresponding to the four augmentation concepts.

Two different approach trajectories were flown. The first trajectory contained three turns of 45 deg and three turns of 30 deg (Fig. 14a). Six flight-path angle changes were implemented as well, with a maximum descent angle of 3 deg (Fig. 14b). The second trajectory was a mirrored version of the first.

The aircraft model used was a nonlinear, level-D model of the Cessna Citation 500, a small twin-engine business jet.[56] The aircraft is simulated with a clean configuration. The airspeed was kept constant at 170 kn (IAS) using an autothrottle. All conditions used a yaw damper.

1. Prediction Time T_p and FBW Lag Time ΔT

Following the same procedure as discussed in Sec. III.B, the optimal lateral FPP predictor time T_p for the airspeed of 170 kn was found to be 3 s. Because of the different aircraft dynamics in the vertical plane, the optimal vertical FPP predictor time was smaller. The FPP predictor symbol cannot be driven by two different predictor times, however. This is a common problem with flight-path predictors and a work-around has been suggested by Grunwald et al.[3] The vertical acceleration that drives the vertical motions of the FPP is multiplied with a gain (here, 0.2) before it is used in the predictor algorithm that uses the optimal predictor time for the lateral control dimension.[42]

The FBW lateral control system lag time ΔT, which determines the time ahead for which the commanded FPV reference frame is displayed (FBW+) was calculated online using Eq. (4). For the 170-kn airspeed, it varied between approximately 1.2 and 1.5 s, resulting in the reference frame moving slightly forward and backward. The questionnaire showed that this remained largely unnoticed by the pilots.

Table 2 Initial intensities of the patchy turbulence velocities (m^2/s^2) and accelerations (m^2/s^4)

Parameter	Value
$\sigma^2_{u_g}$	0.046
$\sigma^2_{v_g}$	0.152
$\sigma^2_{w_g}$	0.164
$\sigma^2_{u_{g\text{asymm}}}$	0.078
$\sigma^2_{w_{g\text{asymm}}}$	0.168
$\sigma^2_{\dot{u}_g}$	0.416
$\sigma^2_{\dot{v}_g}$	1.74
$\sigma^2_{\dot{w}_g}$	1.94

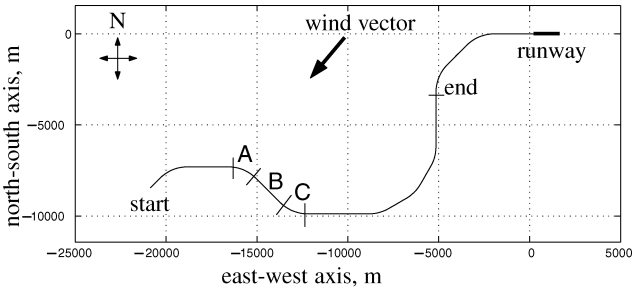

a) Top-down view

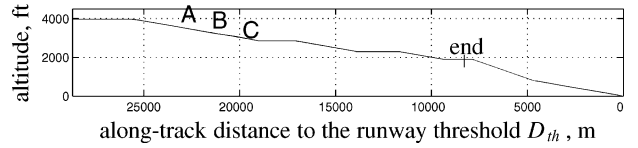

b) Side view

Fig. 14 Experiment trajectory, A–C part of trajectory also shown in Fig. 15, direction of the wind, and start and end indicate where each run started and ended, respectively.

2. Atmosphere Model

The atmospheric turbulence model was a patchy Dryden filter[54] that was also used in a previous study on this subject.[26] The turbulence signals were all generated in advance; their intensities are shown in Table 2. The turbulence intensity for the heavy condition was six times that of the light condition.

A standard wind profile was used, as in earlier study.[26] At 1000 ft, the wind had a velocity of 15 kn, with a direction always at an angle of 45 deg with respect to the localizer plane, in the opposite direction of the landing (Fig. 14).

C. Experiment Hypotheses

Regarding the augmentation concepts, it was hypothesized that the lowest pilot workload and control activity and the best path-following performance would be achieved with the control augmentation (FBW and FBW+). The opposite was hypothesized for the baseline control with FPV, whereas these metrics were expected to rate in between for the FPP. It was hypothesized further that adding the command-FPV reference frame in the control augmentation

condition, that is, FBW+, would improve performance, at the cost, however, of higher workload and more control activity.

Regarding the effects of turbulence intensity, it was hypothesized that higher intensities would reduce performance and increase workload and control activity for the display augmentation concepts (FPV and FPP), whereas they would remain the same for the CAS.

VII. Results and Discussion

A. Results

1. Time Histories

Figures 15a and 15b show typical time histories of lateral control deflections during two curves of the trajectory. With the CAS, the stick needed to be deflected during the curve. Overall, only small corrections were needed with these concepts, whereas with the display augmentation concepts, more stick activity was shown. Superimposing a reference frame (FBW+) resulted in somewhat larger control deflections. The abbreviations, representing the display and control augmentation system combinations, are summarized in Table 3.

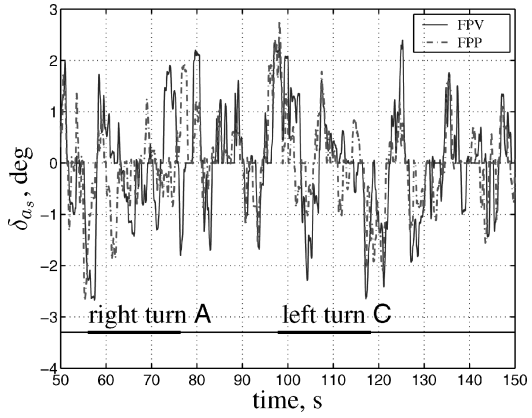

a) Lateral control deflections with FPV and FPP

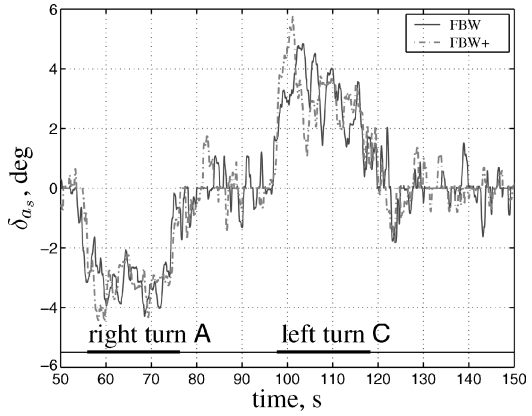

b) Lateral control deflections with FBW and FBW+

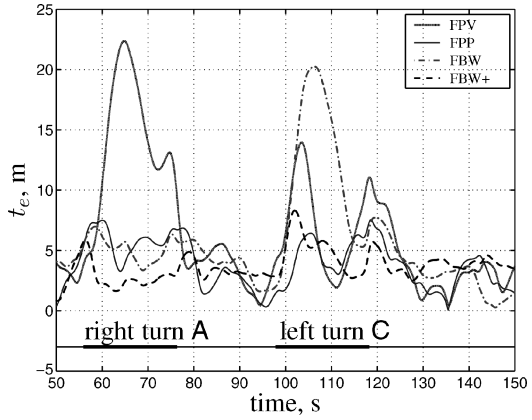

c) All augmentation concepts

Fig. 15 Time histories of lateral stick inputs δ_{a_s} and total position error t_e for all control augmentation concepts (one pilot, heavy turbulence). Including curved sections A–C (thick lines) of trajectory in Fig. 14.

Table 3 Key elements of four display and control system combinations (AC)

AC	Description
FPV	Unaugmented control combined with a FPV symbol.
FPP	Unaugmented control combined with a FPP symbol, together with a transparent predictor reference frame.
FBW	Flight-path-oriented FBW control combined with an instantaneous FPV symbol and a command FPV symbol.
FBW+	Identical to the described FBW, now with a highlighted reference frame for the command FPV symbol.

Figure 15c shows path-following performance expressed in the total position error t_e. The control augmentation (FBW) appears to provide worse performance than the FPP for the left turn, but when the reference frame is added (FBW+), performance becomes almost the same as with the FPP.

2. Path-Following Performance: Position

A full-factorial analysis of variance (ANOVA) was conducted with the AC (four levels) and turbulence (AT) (two levels) as the independent variables (Tables 4 and 5). The means and the 95% confidence limits of the main dependent measures are shown in Figs. 16 and 17.

Position-tracking performance (Fig. 16) was significantly influenced by the augmentation: for x_e, $F_{3,15} = 44.682$ and $p \leq 0.01$; for v_e, $F_{3,15} = 11.689$ and $p \leq 0.01$; and for t_e, $F_{3,15} = 39.453$ and $p \leq 0.01$. A post-hoc analysis [Student Newman-Keuls (SNK), $\alpha = 0.05$] revealed that the basic control (FPV) resulted in the worst performance. Surprisingly, performance with control augmentation was worse than with the FPP; it improved when adding a reference frame (FBW+), confirming the findings from the time history analysis. The best lateral position-tracking performance was achieved with the FPP. The FBW+ yielded the smallest vertical position error.

Although, as was hypothesized, the trends in the data suggest that performance reduces in heavy turbulence for the display augmentation concepts, this effect was not significant. Performance with the control augmentation concepts tends to improve in the heavy turbulence conditions, but again this trend was not significant.

3. Path-Following Performance: Flight-Path Angle

Flight-path tracking performance (Fig. 16) was also significantly affected by the augmentation: for χ_e, $F_{3,15} = 14.468$ and $p \leq 0.01$ and for γ_e, $F_{3,15} = 5.044$ and $p = 0.013$. In light turbulence, the FPP yielded the best performance, followed by the control augmentation concepts; the baseline (FPV) resulted in the worst performance. In heavy turbulence, performance with the FPP decreased considerably, having a significant effect on the vertical flight-path tracking performance: for γ_e, $F_{1,5} = 35.303$ and $p \leq 0.01$. Because performance was only slightly affected by turbulence for the control AC, as was hypothesized, the AC $\times$ AT interaction was significant as well: for χ_e, $F_{3,15} = 4.271$ and $p = 0.023$.

In contrast with the position-tracking performance, it was found that showing the reference frame (the FBW+ concept) decreased flight-path-tracking performance, an effect that was only significant in the vertical dimension (SNK, $\alpha = 0.05$). Apparently, pilots sacrificed flight-path-tracking performance to enhance their position-tracking performance with the FBW+ concept.

4. Control Activity

Control activity (Fig. 16) expressed in the control deflection rates and the control deflection counters, was significantly smaller for the control augmentation concepts, except for the vertical control deflection rates: for $\dot{\delta}_{a_s}$, $F_{3,15} = 19.814$ and $p \leq 0.01$; for dacnt, $F_{3,15} = 6.008$ and $p \leq 0.01$; and for decnt, $F_{3,15} = 4.196$

Table 4 Results of full-factorial ANOVA on dependent measures, regarding path-following performance, pilot physical and mental workload, and accelerations

	Position error			Flight-path angle error		Control activity				Acceleration		Workload
Variable	v_e	x_e	t_e	γ_e	χ_e	$\dot{\delta}_{e_s}$	δ_{a_s}	decnt	dacnt	n_z	$\ddot{x}_e$	zTLX
Main effects												
AC	★★[a]	★★	★★	★[b]	★★	○[c]	★★	★	★★	★★	★★	★★
AT	·	·	·	★★	·	★	★★	★	○	★★	★★	★
Two-way interactions												
AC × AT	·	·	·	○	★	·	★★	★★	★	·	★★	★★

[a]Chance level of $p \le 0.01$. [b]Chance level of $0.01 < p \le 0.05$. [c]Chance level of $0.05 < p \le 0.10$.

Table 5 Results of full-factorial ANOVA on dependent measures, regarding ride comfort and aircraft attitude

	Attitude		Attitude rates		Roll rate counters			Acceleration counters		
Variable	ϕ	θ	$\dot{\phi}$	$\dot{\theta}$	$\dot{\phi}_{3-5}$	$\dot{\phi}_{5-7}$	$\dot{\phi}_{>7}$	Δn_{z_1}	Δn_{z_2}	Δn_{z_3}
Main effects										
AC	★★[a]	★[b]	★★	★	★★	★★	★★	★★	★	★
AT	★★	○[c]	★★	★★	★★	★★	★★	★★	★★	★★
Two-way interactions										
AC × AT	★★	·	★★	★★	★★	★★	★★	★★	★★	·

[a]Chance level of $p \le 0.01$. [b]Chance level of $0.01 < p \le 0.05$. [c]Chance level of $0.05 < p \le 0.10$.

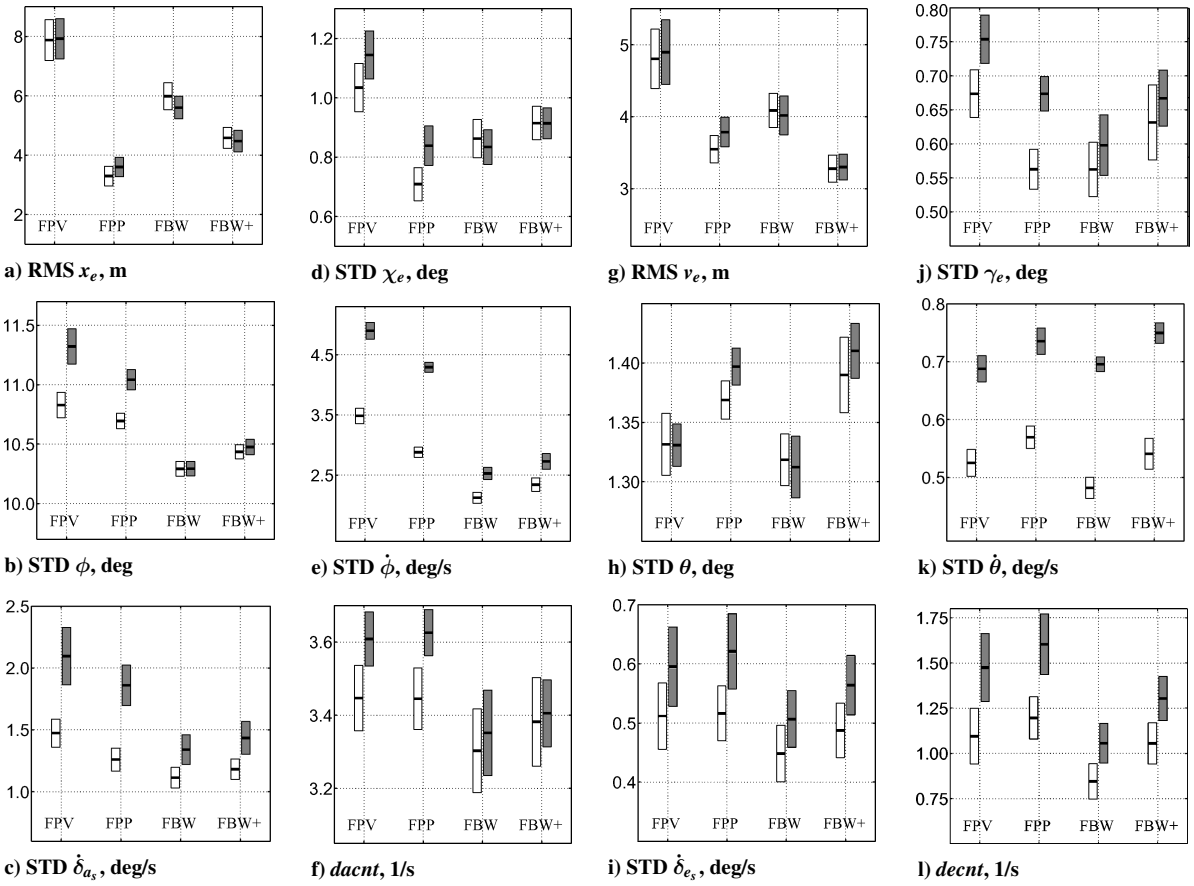

Fig. 16 Means and 95% confidence limits of main dependent measures (all subjects): white bar, light turbulence and gray bar, heavy turbulence.

and $p = 0.024$. Post-hoc analyses (SNK, $\alpha = 0.05$) confirmed these findings, supporting our hypotheses. The effects are stronger in the lateral dimension. Adding the command FPV reference frame (FBW+) resulted in a slight but statistically significant increase in control activity.

For all AC, control activity increased significantly for the heavy turbulence conditions, except for the lateral control deflection counters. However, the increase was stronger for the display augmentation concepts than for the control augmentation concepts (in particular for the lateral control), as was hypothesized, causing significant two-way interactions AC × AT: for $\dot{\delta}_{a_s}$, $F_{3,15} = 17.237$ and $p \le 0.01$; for dacnt, $F_{3,15} = 3.664$ and $p = 0.037$; and for decnt, $F_{3,15} = 5.443$ and $p \le 0.01$.

5. *Aircraft Attitude and Attitude Rates*

The attitude angles, attitude rates (Fig. 16), and roll-rate counters (Fig. 17) were all highly affected by the experiment conditions.

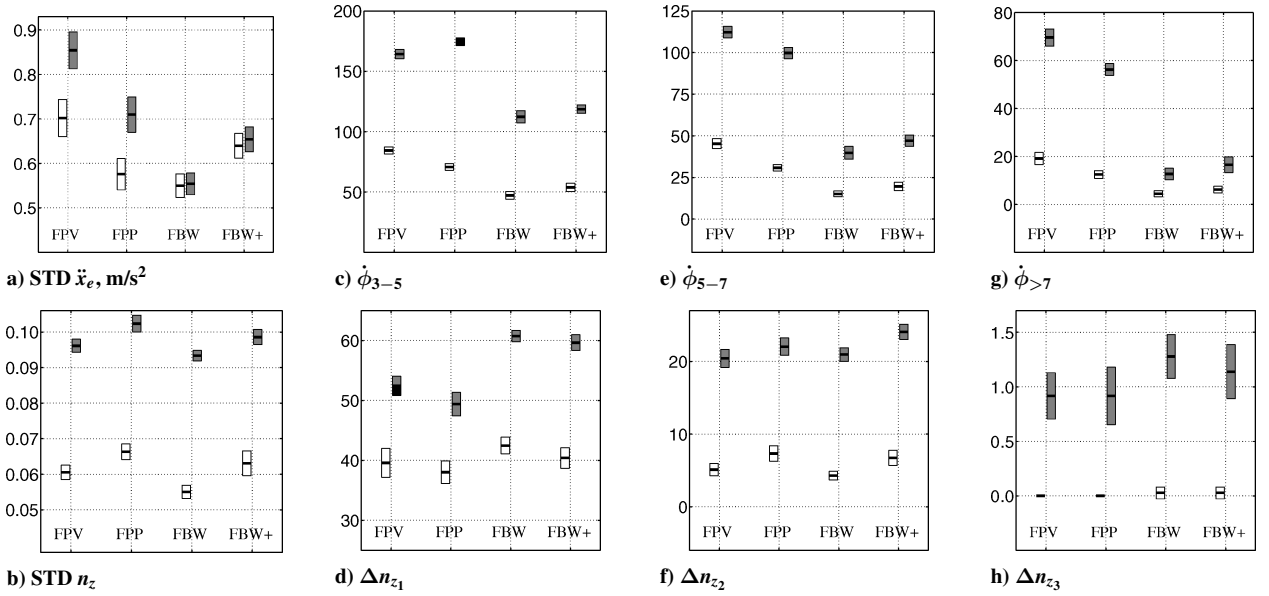

Fig. 17 Means and 95% confidence limits of measures related to ride comfort (all subjects): white bar, light turbulence and gray bar heavy turbulence.

Independent of turbulence intensity, the lowest values were found for the control augmentation. In the lateral dimension, the highest values were found for the baseline control (FPV); for the vertical control, the peaks were found for the FPP. These effects were all significant. The addition of the command FPV reference frame (FBW+ condition) led to an increase in attitude variability.

The heavy turbulence led to a significant increase of these dependent measures, except for the pitch angle. As hypothesized, these effects were much stronger for the display augmentation concepts as compared to the control augmentation, yielding highly significant two-way interactions AC × AT: for $\dot{\phi}$, $F_{3,15} = 28.956$ and $p \leq 0.01$; for $\dot{\phi}$, $F_{3,15} = 221.007$ and $p \leq 0.01$; for $\dot{\theta}$, $F_{3,15} = 8.397$ and $p \leq 0.01$; for $\dot{\phi}_{3-5}$, $F_{3,15} = 38.349$ and $p \leq 0.01$; for $\dot{\phi}_{5-7}$, $F_{3,15} = 240.876$ and $p \leq 0.01$; and for $\dot{\phi}_{>7}$, $F_{3,15} = 214.444$ and $p \leq 0.01$. The only exception to this finding was for the STD of pitch rate, which increased significantly for the FBW concepts.

6. Ride Comfort

Most of the lateral accelerations and the n_z counters (Fig. 17) were significantly influenced by the AC: for $\ddot{x}_e$, $F_{3,15} = 16.790$ and $p \leq 0.01$; for n_z, $F_{3,15} = 6.776$ and $p \leq 0.01$; for Δn_{z_1}, $F_{3,15} = 13.144$ and $p \leq 0.01$; for Δn_{z_2}, $F_{3,15} = 5.306$ and $p = 0.011$; and for Δn_{z_3}, $F_{3,15} = 3.294$ and $p = 0.050$. Independently of turbulence intensity, the FBW concept resulted in the smallest accelerations, as was hypothesized. The accelerations increased when the reference frame was added (FBW+). Surprisingly, the lateral accelerations with the FPP were quite similar. With the control augmentation, the normal acceleration counters were higher in the lower region, Δn_{z_1}, whereas in the higher regions, all systems were similar.

The acceleration metrics increased significantly in heavy turbulence, but the significant interaction AC × AT shows that this effect was not found for the lateral acceleration for the control augmentation; $F_{3,15} = 12.247$ and $p \leq 0.01$.

7. Pilot Workload

Workload ratings (Fig. 18) support the trends in the data. Significant effects of the augmentation, $F_{3,15} = 12.124$ and $p \leq 0.01$, and turbulence, $F_{1,5} = 7.526$ and $p = 0.041$, were found. In the light turbulence, the FPP and the control augmentation concepts yield the same workload. In the heavy turbulence condition, however, workload with the FPP increased significantly. Overall, workload is highest for the baseline control (FPV). Adding the reference frame to the FBW slightly increased workload.

As was hypothesized, for the higher turbulence intensity, workload with the display augmentation concepts increased, whereas it remained the same for the control augmentation concepts, causing the significant two-way interaction, $F_{3,15} = 7.214$ and $p \leq 0.01$.

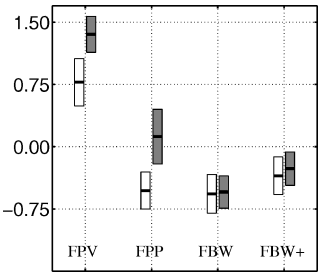

Fig. 18 Means and 95% confidence limits of normalized TLX workload ratings (all subjects): white bar, light turbulence; and gray bar, heavy turbulence.

8. Pilot Questionnaire

Pilots commented that flying with the FPP resembled the task with an FD and, surprisingly, they reported a decrease of situation awareness. They reported that the predictor and reference frame captured their attention and made them less concerned with keeping the "big picture." However, they did find the FPP concept a very pleasant way of flying. The control augmentation concepts (FBW and FBW+) were reported to result in a quite relaxed way of flying: Pilots trusted the FBW controller to keep the commanded path and mitigate the effects of turbulence.

Following the curved parts of the trajectory, however, remained a cause of concern. Although adding the commanded FPV reference frame (FBW+) helped, pilots found it to be positioned too close ahead to be efficient. Pilots recommended using a smaller frame, or a symbol marking the center of the frame. In hindsight, the reference frame could better have been presented at twice the FBW control lag, $2\Delta T$, as suggested earlier. A later study supported this finding.[31]

B. Discussion

As was hypothesized, the FPP and the flight-path-oriented control augmentation concepts significantly improved pilot path-following performance and reduced workload with respect to the baseline manual control. However, the result that performance was similar for these concepts was unexpected, because the analysis showed a clear superiority of the control augmentation. This can be attributed to the limited scope of the theoretical analysis, which only considered straight flight, whereas the experiment included curves.

The theoretical analysis emphasizes in particular disturbance rejection, in which control augmentation is clearly superior. It did not consider the main strength of the FPP over the control augmentation configuration, that is, that it allows for anticipating future changes in

the nominal trajectory. In the pilot-in-the-loop experiment, in which a complex curved trajectory was followed, the performance of the AC converged to a similar level. Another possible explanation is that pilots kept performance at the same level, but at the cost of workload and control activity.

As was hypothesized, the control augmentation concepts yielded the best flight-path-tracking performance, the lowest pilot control activity, the lowest workload, and the most comfortable ride. Position-tracking performance can be further improved by providing a reference frame for the commanded FPV, at the cost, however, of a slightly higher control activity and workload.

The display augmentation concepts were more strongly affected by the turbulence conditions: Pilot control activity and workload were increased when this property of the pilot task difficulty increased. Path-following performance remained the same. As hypothesized, for the control augmentation systems, the pilot performance, workload, and control activity were only slightly affected by the turbulence intensity.

In the present experiment, pilots had only a single task and could focus all of their attention on optimizing performance in the aircraft guidance task, and this may have resulted in a too positive view of the FPP display augmentation. The main disadvantage of display augmentation lies in that pilots must continuously compensate for the effects of atmospheric disturbances acting on the vehicle, a task that requires a high level of attention. Future experiments should shed a light on this issue, and it is recommended to repeat the experiment discussed here in a high workload situation, in which pilots have to share their attention between the aircraft guidance task and other cognitive tasks.

VIII. Conclusions

The FPP display augmentation and the flight-path-oriented control augmentation both significantly improve pilot path-following performance with perspective flight-path displays, while at the same time reducing workload with respect to the baseline manual control. Although the FPP provides the best position-tracking performance, the control augmentation resulted in the best flight-path-tracking performance, the lowest pilot control activity, the lowest workload, and a more comfortable ride. Position-tracking performance with the flight-path-oriented control augmentation can be further improved by providing a reference frame for the commanded FPV. Pilot workload and control activity with the display augmentation concepts were strongly affected by the task difficulty measure of atmospheric turbulence intensity. Performance, however, remained the same. With control augmentation, pilot performance, workload, and control activity were not affected by the turbulence intensity. Hence, the benefits of control augmentation over display augmentation are likely to become more clear in high-workload situations, in which pilots have other responsibilities besides manual aircraft control.

Acknowledgments

The authors wish to thank the staff of the SIMONA Research Simulator of the Delft University of Technology and, in particular, Olaf Stroosma for his assistance in the operation of SIMONA. The authors also wish to thank all pilots who participated in the experiment.

References

[1]Mulder, J. A., Van Paassen, M. M., and Mulder, M., "Perspective Guidance Displays Show the Way Ahead," *Journal of Aerospace Computing, Information and Communication*, Vol. 1, No. 11, 2004, pp. 428–431.

[2]Wilckens, V., "On the Dependence of Information Display Quality Requirements Upon Human Characteristics and 'Pilot/Automatics'-Relations," *Proceedings of the Seventh Annual Conference on Manual Control*, NASA SP-281, 1971, pp. 177–183.

[3]Grunwald, A. J., Robertson, J. B., and Hatfield, J. J., "Evaluation of a Computer-Generated Perspective Tunnel Display for Flight-Path Following," NASA TP-1736, Dec. 1980.

[4]Roscoe, S. N., and Jensen, R. S., "Computer-Animated Predictive Displays for Microwave Landing Approaches," *IEEE Transactions on Systems, Man, and Cybernetics*, Vol. SMC-11, No. 11, 1981, pp. 760–765.

[5]Grunwald, A. J., "Tunnel Display for Four-Dimensional Fixed-Wing Aircraft Approaches," *Journal of Guidance and Control*, Vol. 7, No. 3, 1984, pp. 369–377.

[6]Sachs, G., "Perspective Predictor/Flight-Path Display with Minimum Pilot Compensation," *Journal of Guidance, Control, and Dynamics*, Vol. 23, No. 3, 2000, pp. 420–429.

[7]Parrish, R. V., Busquets, A. M., Williams, S. P., and Nold, D. E., "Spatial Awareness Comparisons Between Large-Screen, Integrated Pictorial Displays and Conventional EFIS Displays During Simulated Landing Approaches," NASA TP-3467, NASA, Oct. 1994.

[8]Regal, D., and Whittington, D., "Guidance Symbology for Curved Flight Paths," *Proceedings of the Eighth International Symposium on Aviation Psychology*, The Ohio State Univ., Columbus, OH, 1995, pp. 74–79.

[9]Williams, K. W., "Impact of Aviation Highway-in-the-Sky Displays on Pilot Situation Awareness," Technical Rept. DOT/FAA/AM-00/31, Federal Aviation Administration Civil Aeromedical Inst., Oklahoma City, OK, 2000.

[10]Funabiki, K., "Tunnel-in-the-Sky Display Enhancing Autopilot Mode Awareness," *Conference Proceedings of the 1997 CEAS Free Flight Symposium*, National Aerospace Laboratory, Amsterdam, 1997, pp. 29.1–29.11.

[11]Beringer, D. B., "Development of Highway-in-the-Sky Displays for Flight-Path Guidance: History, Performance Results, Guidelines," *Proceedings of the 44th Annual Meeting of the Human Factors & Ergonomics Society*, Human Factors and Ergonomics Society, Santa Monica, CA, 2000, pp. 3.21–3.24.

[12]Grunwald, A. J., Robertson, J. B., and Hatfield, J. J., "Experimental Evaluation of a Perspective Tunnel Display for Three-Dimensional Helicopter Approaches," *Journal of Guidance and Control*, Vol. 4, No. 6, 1981, pp. 623–631.

[13]Barrows, A. K., Enge, P., Parkinson, B. W., and Powell, J. D., "Flight Tests of a 3-D Perspective-View Glass-Cockpit Display for General Aviation," *Proceedings of the Institute of Navigation GPS-95 Meeting*, Institute of Navigation, Alexandria, VA, 1995, pp. 1615–1622.

[14]Below, C., von Viebahn, H., and Purpus, M., "Flight Tests of The 4D Flight Guidance Display," *Proceedings of the SPIE Technical Conference Synthetic Vision for Vehicle Guidance and Control, Aerosense*, Vol. 3088, Society of Photo-Optical Instrumentation Engineers, Bellingham, WA, 1997, pp. 74–79.

[15]Funabiki, K., Muraoka, K., Terui, Y., Harigae, M., and Ono, T., "In-Flight Evaluation of Tunnel-in-the-Sky Display and Curved Approach Pattern," *Proceedings of the AIAA Guidance, Navigation and Control Conference,* AIAA Reston, VA, 1999, pp. 108–114.

[16]Mulder, M., Kraeger, A. M., and Soijer, M. W., "Delft Aerospace Tunnel-in-the-Sky Flight Tests," AIAA Paper 2002-4929, Aug. 2002.

[17]Grunwald, A. J., and Merhav, S. J., "Effectiveness of Basic Display Augmentation in Vehicular Control by Visual Field Cues," *IEEE Transactions on Systems, Man, and Cybernetics*, Vol. SMC-8, No. 9, 1978, pp. 679–690.

[18]Grunwald, A. J., "Predictor Laws for Pictorial Flight Displays," *Journal of Guidance and Control*, Vol. 8, No. 5, 1985, pp. 545–552.

[19]Mulder, M., "Flight-Path Vector Symbology in a Tunnel-in-the-Sky Display," *Proceedings of the XVIIIth European Annual Conference on Human Decision Making and Manual Control*, Loughborough Univ., Loughborough, U.K., 1999, pp. 250–267.

[20]Grunwald, A. J., "Improved Tunnel Display for Curved Trajectory Following: Control Considerations," *Journal of Guidance, Control, and Dynamics,* Vol. 19, No. 2, 1996, pp. 370–377.

[21]Funabiki, K., Iijima, T., and Nojima, T., "Evaluation of a Trajectory-Based Operations Concept for Small Aircraft: Airborne Aspect," *Proceedings of the IEEE/AIAA Digital Avionics Systems Conference*, IEEE Press, Piscataway, NJ, 2003, pp. 12.C.5.1–12.C.5.11.

[22]Mulder, M., "An Information-Centered Analysis of the Tunnel-in-the-Sky Display, Part One: Straight Tunnel Trajectories," *International Journal of Aviation Psychology*, Vol. 13, No. 1, 2003, pp. 49–72.

[23]Newman, R. L., and Mulder, M., "Pathway Displays a Literature Review," *Proceedings of the 22nd Digital Avionics Systems Conference*, IEEE Press, Piscataway, NJ, 2003, pp. 9.D.6–1–9.D.6–10.

[24]Prinzel, L. J., Comstock, J. R., Glaab, L. J., Kramer, L. J., Arthur, J. J., and Barry, J. S., "The Efficacy of Head-Down and Head-Up Synthetic Vision Display Concepts for Retro- and Forward-Fit of Commercial Aircraft," *The International Journal of Aviation Psychology,* Vol. 14, No. 1, 2004, pp. 53–77.

[25]Schnell, T., Kwon, Y., Merchant, S., and Etherington, T., "Improved Flight Technical Performance in Flight Decks Equipped with Synthetic Vision Information System Displays," *The International Journal of Aviation Psychology*, Vol. 14, No. 1, 2004, pp. 79–102.

[26]Mulder, M., Veldhuijzen, A. R., Van Paassen, M. M., and Mulder, J. A., "Integrating Fly-by-Wire Controls with Perspective Flight-Path Displays," *Journal of Guidance, Control and Dynamics*, Vol. 28, No. 6, 2005, pp. 1263–1274.

[27]Lambregts, A. A., and Cannon, D. G., "Development of a Control Wheel Steering Mode and Suitable Displays that Reduce Pilot Workload and Improve Efficiency and Safety of Operation in the Terminal Area and in Windshear," *Proceedings of the AIAA Guidance, Navigation and Control Conference*, AIAA, New York, 1979, pp. 609–620.

[28]Stewart, E. C., Ragsdale, W. A., and Wunschel, A. J., "An Evaluation of Automatic Control System Concepts for General Aviation Airplanes," *Proceedings of the AIAA Atmospheric Flight Mechanics Conference*, AIAA New York, 1988, pp. 330–343.

[29]Stewart, E. C., "A Piloted Simulation Study of Advanced Controls and Displays for Novice General Aviation Pilots," AIAA Paper 94-0276, Jan. 1994.

[30]Duerksen, N., "Advanced Flight Controls and Pilot Displays for General Aviation," *Proceedings of the AIAA/ICAS International Air and Space Symposium and Exposition: The Next 100 Years*, AIAA Paper 2003-2647, 2003.

[31]Borst, C., Mulder, M., and Van Paassen, M. M., "Fly-by-Wire and Tunnel-in-the-Sky Displays: Development and Experimental Evaluation of a Path-Oriented Control Augmentation," AIAA Paper 2004-5236, Aug. 2004.

[32]Mulder, M., and Mulder, J. A., "A Cybernetic Analysis of Perspective Flight-Path Display Dimensions," *Journal of Guidance, Control and Dynamics*, Vol. 28, No. 3, 2005, pp. 398–411.

[33]Gold, T., "Quickened Manual Flight Control with External Visual Guidance," *IEEE Transactions on Aerospace and Navigational Electronics*, Vol. ANI-11, No. 9, 1965, pp. 151–156.

[34]Hynes, C. S., Franklin, J. A., Hardy, G. H., Martin, J. L., and Innis, R. C., "Flight Evaluation of Pursuit Displays for Precision Approach of Powered-Lift Aircraft," *Journal of Guidance*, Vol. 12, No. 4, 1989, pp. 521–529.

[35]Jensen, R. S., "Prediction and Quickening in Perspective Flight Displays for Curved Landing Approaches," *Human Factors*, Vol. 23, No. 3, 1981, pp. 355–363.

[36]Schmitt, V. R., Morris, J. W., and Jenney, G. D., *Fly-by-Wire: A Historical and Design Perspective*, Society of Automotive Engineers, Warrendale, PA, 1998.

[37]Eberts, R. E., "Internal Models, Tracking Strategies, and Dual-Task Performance," *Human Factors,* Vol. 29, No. 4, 1987, pp. 407–419.

[38]Newman, R. L., *Head-Up Displays: Designing the Way Ahead*, Avebury Aviation, Aldershot, U.K., 1995.

[39]Grunwald, A. J., and Kohn, S., "Flight-Path Estimation in Passive Low-Altitude Flight by Visual Cues," *Journal of Guidance, Control, and Dynamics*, Vol. 16, No. 2, 1993, pp. 363–370.

[40]McRuer, D. T., and Jex, H. R., "A Review of Quasi-Linear Pilot Models," *IEEE Transactions on Human Factors in Electronics*, Vol. HFE-8, No. 3, 1967, pp. 231–249.

[41]Poulton, E. C., *Tracking Skill and Manual Control*, Academic Press, London, 1974.

[42]Lam, T. M., "A Comparative Study Between Display Augmentation and Control Augmentation for Tunnel-in-the-Sky Displays," M.Sc. Thesis, Faculty of Aerospace Engineering, Delft Univ. of Technology, Delft, The Netherlands, Oct. 2003.

[43]Mulder, M., Chiecchio, J., Pritchett, A. R., and Van Paassen, M. M., "Testing Tunnel-in-the-Sky Displays and Flight Control Systems with and Without Flight Simulator Motion," *Proceedings of the 12th International Symposium on Aviation Psychology*, Wright State Univ., Dayton, OH, 2003, pp. 839–844.

[44]Kelley, W. W., "Simulator Evaluation of a Flight-Path Angle Control System for a Transport Airplane with Direct Lift Control," NASA TP-1116, NASA, March 1978.

[45]Miller, G. K., Jr., "Fixed-base Simulation Study of Decoupled Longitudinal Controls During Approach and Landing of a Medium Jet Transport in the Presence of Windshear," NASA TP-1519, NASA, Oct. 1979.

[46]Steinmetz, G. G., "Simulation Development and Evaluation of an Improved Longitudinal Velocity Vector Control-Wheel Steering Mode and Electronic Display Format," NASA TP-1664, NASA, Aug. 1980.

[47]Sankrithi, M. K. V., and Bryant, W. F., "7J7 Manual Flight Control Functions," *Proceedings of the AIAA Guidance, Navigation and Control Conference*, AIAA, New York, 1987, pp. 905–913.

[48]Beringer, D. B., "Performance-controlled Systems, Fuzzy Logic, and Fly-by-Wire Controls: Revisiting Applications to General Aviation," *Proceedings of the 43rd Annual Meeting of the Human Factors & Ergonomics Society*, Human Factors and Ergonomics Society, Santa Monica, CA, 1999, pp. 61–65.

[49]Mulder, M., "An Information-Centered Analysis of the Tunnel-in-the-Sky Display, Part Two: Curved Tunnel Trajectories," *International Journal of Aviation Psychology*, Vol. 13, No. 2, 2003, pp. 131–151.

[50]Bergman, C. A., "An Airplane Performance Control System: A Flight Experiment," *Human Factors,* Vol. 18, No. 2, 1976, pp. 173–182.

[51]Roscoe, S. N., Eisele, J. E., and Bergman, C. A., "Advanced Integrated Aircraft Displays and Augmented Flight Control," *Scientific Findings*, Vol. 1, ADA022459, Inst. of Aviation, Univ. of Illinois, Urbana, IL, June 1975, pp. 1–44.

[52]Hardy, G. H., "Pursuit Display Review and Extension to a Civil Tilt Rotor Flight Director," AIAA Paper 2002-4925, Aug. 2002.

[53]Moralez, E., III, Tucker, G. E., Hindson, W. S., Frost, C. R., and Hardy, G. H., "In-Flight Assessment of a Pursuit Guidance Display Format for Manually Flown Precision Instrument Approaches," *Proceedings of the American Helicopter Society 60th Annual Forum*, American Helicopter Society, Alexandria, VA, 2004, pp. 1749–1761.

[54]Van de Moesdijk, G. A. J., "The Description of Patchy Atmospheric Turbulence, Based on a Non-Gaussian Simulation Technique," Faculty of Aerospace Engineering, Rept. LR-192, Delft Univ. of Technology, Delft, The Netherlands, Feb. 1975.

[55]Hart, S. G., and Staveland, L. E., "Development of NASA-TLX (Task Load Index): Results of Empirical and Theoretical Research," *Human Mental Workload*, edited by P. A. Hancock and N. Meshkati, Elsevier Science, Amsterdam, 1988, pp. 139–183.

[56]Van der Linden, C. A. A. M., "DASMAT: The Delft University Aircraft Simulation Model and Analysis Tool," Faculty of Aerospace Engineering, Rept. LR-781, Delft Univ. of Technology, Delft, The Netherlands, April 1996.